Evolution of the Digital Society Reveals Balance between Viral and Mass Media Influence

Kaj-Kolja Kleineberg and Marián Boguñá

Departament de Física Fonamental, Universitat de Barcelona,
Martí i Franquès 1, 08028 Barcelona, Spain

Online social networks (OSNs) enable researchers to study the social universe at a previously unattainable scale. The worldwide impact and the necessity to sustain the rapid growth of OSNs emphasize the importance of unraveling the laws governing their evolution. Empirical results show that, unlike many real-world growing networked systems, OSNs follow an intricate path that includes a dynamical percolation transition. In light of these results, we present a quantitative two-parameter model that reproduces the entire topological evolution of a quasi-isolated OSN with unprecedented precision from the birth of the network. This allows us to precisely gauge the fundamental macroscopic and microscopic mechanisms involved. Our findings suggest that the coupling between the real preexisting underlying social structure, a viral spreading mechanism, and mass media influence govern the evolution of OSNs. The empirical validation of our model, on a macroscopic scale, reveals that virality is 4–5 times stronger than mass media influence and, on a microscopic scale, individuals have a higher subscription probability if invited by weaker social contacts, in agreement with the "strength of weak ties" paradigm.

I. INTRODUCTION

The rapid growth of online social networks (OSNs), like Twitter or Facebook, is reshaping the social landscape and changing the way humans interact on a worldwide scale. Needless to say, social networks existed well before OSNs were even invented. However, OSNs offer us the unprecedented opportunity to map social interactions at a scale that was unattainable before the digital era. This has transformed OSNs into huge sociological laboratories, boosting social sciences up to the level of experimental sciences. There is, however, an important difference between traditional social networks and OSNs. Technology-mediated social interactions constitute accelerating phenomena already observed in conventional social networks. Nevertheless, in the case of OSNs, these take place faster and on a worldwide scale. This is already changing the way companies try to promote or sell their products with viral marketing campaigns [1–4], the way influential people, e.g., politicians, interact with their followers on Twitter [5–7], or the way people self-organize and cooperate in protest movements [8,9], crowdfunding [10], etc.

Nonetheless, this sociotechnological revolution must come along with the development of new technologies able to sustain its growth. In this respect, one important issue concerns the design of the basic architecture of current OSNs. The best way to solve the scalability limitations of OSNs is to replace their centralized architecture by a fully decentralized one [11]. This can address privacy considerations and improve service scalability, performance, and fault tolerance in the presence of an expanding base of users and applications. However, to accomplish this program successfully, it is necessary to take into account the social structure of the underlying society and how it interacts with the system, a task that involves network, computer, and social sciences.

As a matter of fact, we already have a fairly good knowledge of the topological properties of the "social graph" among users of OSNs [12–14]. Indeed, large data sets of OSNs have allowed researchers to characterize their topology and validate many principles from the social sciences, such as the "six degrees of separation" [15–19] by Milgram or the "strength of weak ties" by Granovetter [20–25]. However, these results concern static snapshots of the system and, thus, offer little insight into the fundamental mechanisms leading to the evolution of OSNs. Such insights can only be obtained from a detailed analysis of the temporal evolution of topologies of OSNs [26–32]. As we show, in the case of real OSNs, such temporal evolution follows an intricate path: an initial phase where the social graph is made of small clusters with increasing diameter and average degree, followed by a dynamical percolation transition and, finally, an epoch of increasing average degree and shrinking diameter, akin to the observations by Leskovec, Kleinberg, and Faloutsos in Refs. [33,34]. Interestingly, this type of history cannot be explained by

standard models of growing networks under preferential attachmentlike mechanisms, thus calling for new fundamental principles.

In this paper, we focus on a particularly important case study, the Slovakian OSN "Pokec" [35]. This network has a combination of unique properties that make it the perfect test bed for our purposes, namely, the following. (i) It is the most popular friendship-oriented OSN in the country. (ii) Its size represents 25% of the country's population. However, a simple demographic analysis of both the country and Pokec users suggests that, with its current size, it is covering a large fraction of the population susceptible to ever participating in OSNs. (iii) The Slovak language is mostly spoken within the country. (iv) We can reconstruct its temporal evolution since its birth. As a result, we have the full history of a quasi-isolated OSN whose final state is also a good proxy for its underlying offline friendship network. We hypothesize that the underlying social structure is essential for the emergence of OSNs. Under this premise, we introduce a simple model that incorporates viral dynamics and mass media influence [36] operating on a multiplex network [37] formed by online and offline social graphs. The model reproduces very well the topological evolution of the Pokec OSN. Nevertheless, the perfect match is only achieved by introducing into the model the "importance of weak ties" paradigm, yet another empirical evidence in support of Granovetter's theory.

II. RESULTS

A. Evolution of the OSN Pokec: An example of a dynamical percolation transition

Pokec is by far the largest and most popular friendship-oriented OSN in Slovakia [35]. By April of 2012, it gathered around 1.6×10^6 users and 30×10^6 directed friendship relations. Nevertheless, not all directed links correspond to a real social tie: Alice might consider Bob as her friend while Bob may not have the same consideration for Alice. Thus, we discard all nonbidirectional links from the original graph and treat those left as undirected edges. The resulting filtered network is composed of 1.2×10^6 users and 8.3×10^6 bidirectional friendship connections. Interestingly, available users' profile data contains the registration date of all users. Using this information, we can replay the history of the network topology by assuming that an edge between two users exists at a certain time if both users exist at that time. This approximation is reasonable due to observations from, e.g., Ref. [27], which suggests that most edges are created in a short time period after the birth of its end nodes.

In the inset of Fig. 1, we show the temporal evolution of the number of registered users. We clearly appreciate a sustained monotonic increase, suggesting that the popularity of Pokec has not diminished even after the onset of Facebook in the year 2004. This monotonic relationship allows us to use the number of current users $N(t)$ as a measure of time instead of the physical time t. While this is
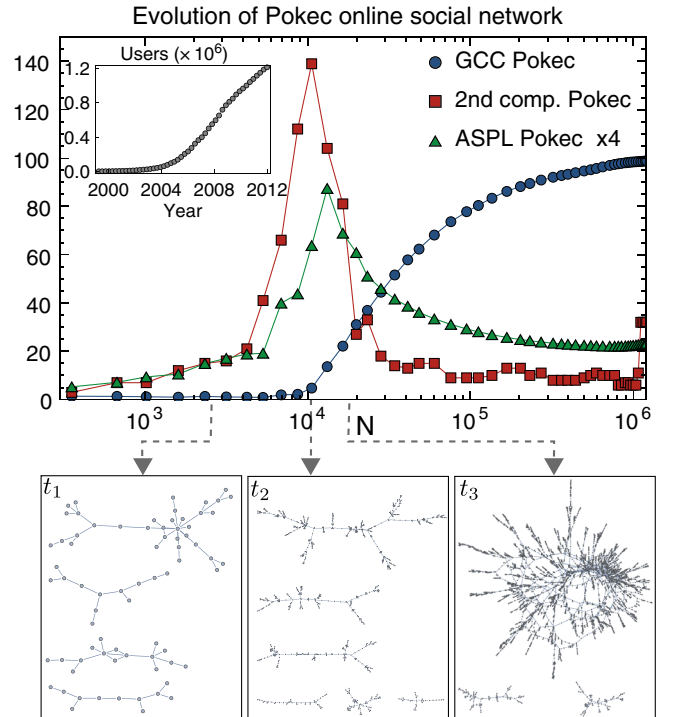

FIG. 1. Topological evolution of the empiric network. Top: The inset shows the evolution of the network size from 1999 to 2012. The main plot shows the relative size of the GCC (blue circles), the size of the second largest component (red squares), and the average shortest path length (green triangles, multiplied by 4 for better readability). Bottom: The largest components of the network are visualized at three different times, before the critical point t_1, at the critical point t_2, and after it, t_3.

only a rescaling of the temporal axis, it makes the comparison with models easier. The main plot in Fig. 1 shows the evolution of the giant connected component (GCC) as a function of the network size. We observe a behavior that could be interpreted as a dynamical phase transition between a phase that consists of small disconnected clusters and a percolated phase where a macroscopic fraction of the network (99% at the end of the evolution) is connected. In percolation theory, the signature of such a continuous transition is encoded in the divergence, at the critical point, of the susceptibility χ, defined as a measure of the ensemble fluctuations of the size of the GCC. Unfortunately, this technique cannot be applied in our case, as the temporal evolution of the Pokec social graph is just one realization of the process. An alternative of the susceptibility is the size of the second largest connected component. This measure is known to diverge at the critical point, and, in a single realization of a finite system, it shows a maximum close to the critical percolation point.

Figure 1 shows a clear peak in the size of the second largest connected component, indicating that, indeed, we are observing a dynamical phase transition [38]. In the same figure, we also show the behavior of the average

shortest path length (ASPL) within the largest connected component, which shows a quite interesting behavior. During the first stage of the evolution, the ASPL increases with the network size, but its growth is not compatible with a logarithmic law, as predicted by the small-world effect. Shortly after the critical point, the ASPL reaches its maximum and then decreases while the size and the average degree [see Fig. 5(b)] of the network increase. At long times, the ASPL reaches a value of about 5, which is compatible with the small-world effect. This behavior was first observed in Ref. [33].

B. Basic model: Balance between virality and mass media influence

Growing network models based on preferential attachment [40] or similar mechanisms [41–48] were designed to describe systems whose functionality is essentially determined by their large-scale connectivity, for example, the physical Internet, power grid networks, biological networks, road networks, etc. Consequently, such models do not show dynamical percolation transitions, as they generate a giant connected component from the very beginning of the network evolution, a constant average degree, and an increasing average shortest path length as a function of the number of nodes. In this type of model, the pool of new nodes that are added to the system does not have any previous relation with existing nodes and the connections of newborn nodes to existing nodes are decided exclusively as a function of the current topological state of the network. However, in the case of friendship-oriented networks, there is a preexisting underlying offline social network conditioning the growth of the OSN. Following this line of reasoning, we conjecture that the observed evolution is the result of a dynamical process that triggers potential users from the offline social network to subscribe to the OSN. Under this assumption, nearly all dynamics able to induce the recruitment of all potential users will yield a dynamical percolation transition. Yet, different dynamics induce different temporal orders in the evolution of OSNs and, therefore, different topological histories.

Following these ideas, we design a two-layer multiplex model for the evolution of OSNs. The upper layer represents the online social network, whereas the bottom layer represents the offline social network. The latter can be considered the subgraph of all *a priori* susceptible individuals from the aggregation of all social interactions between individuals. Each individual can be in three different states depending on whether they are or are not enrolled in the OSN. Susceptible individuals are those not in the OSN but that might eventually become members of it. Active individuals belong to the OSN and are actively using it for their social interactions. Passive individuals also belong to the OSN but are not currently using it to interact with their social contacts; see Fig. 2. The populations of susceptible, active, and passive individuals are governed by
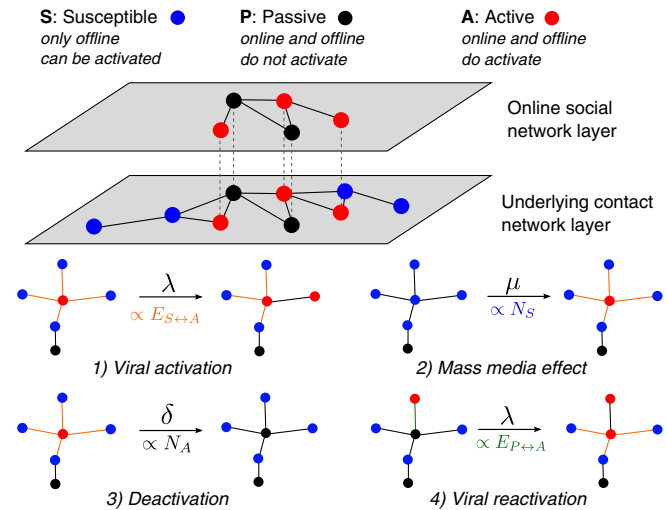

FIG. 2.   Illustration of the two-layer model. The upper layer represents the online social network and contains the active and passive nodes. The bottom layer corresponds to the underlying contact network, which contains all nodes. The four dynamical processes are shown in topological illustrations below.

a combination of an epidemiclike process between active users and susceptible or inactive ones and a mass media effect that equally affects the population of susceptible individuals. There are four possible events. (1). *Viral activation.* A susceptible node can be virally activated and added to the OSN by contact with an active neighbor in the traditional offline network. This event happens at rate λ per each active link. (2). *Mass media effect.* Each susceptible individual becomes active spontaneously at rate μ and is added to the OSN layer as a response to the visibility of the OSN. (3). *Deactivation.* Active users become spontaneously passive at rate δ and no longer trigger viral activations nor reactivate other passive nodes. (4). *Viral reactivation.* At rate λ an active user can reactivate a passive neighbor. The neighbor then becomes active and can trigger both viral activations and viral reactivations. We can arbitrarily set $\delta = 1$, which defines the time scale in units of the deactivation time. The model is then left with two independent parameters, the virality parameter λ and the mass media parameter μ. Finally, newborn users explore the OSN and connect to all their neighbors in the traditional offline social network that, at the time of the subscription, are either active or passive. In the Supplemental Material [39], we conduct an experiment to show that the impact of delayed edge formation can be neglected for reasonable time scales. It is worth pointing out that the dynamics between active and passive users is equivalent to the susceptible-infected-susceptible epidemic model [49]. As happens in the susceptible-infected-susceptible model, our model also has a critical rate λ_c below which the number of active users vanishes whereas above it the activity of the OSN is self-sustained. This makes the model extremely versatile, as it can explain the different fates of OSNs.

We also note that a mean-field version of this dynamics has been recently and independently proposed to model users' activity of OSNs [50].

The viral activation and the mass media effect play complementary roles in terms of their impact on the topological growth of the network. The mass media effect is very likely to create new components especially at the beginning of the network evolution, whereas the viral activation leads to the growth of already existing components. The interplay between these complementary principles is the fingerprint of the evolution of the online social network, and the balance between these mechanisms governs the appearance of the phase transition. We quantify and discuss this balance herein.

Unfortunately, the rigorous validation of the model requires the precise knowledge of the topology of the underlying social network. However, in the particular case of the Pokec network, its large coverage among the subgraph of potential users suggests that we can consider the final snapshot of the Pokec OSN as a good proxy for the real underlying social network. Following this approach, we perform extensive numerical simulations of our model and compare the resulting evolution with the one we observe in the Pokec OSN. Of course, the real evolution of the Pokec network is still ongoing and, thus, we expect this approximation to fail as we approach the final size of the network. In particular, we do not expect the model to reproduce the network growth in physical time because, as the model approaches the size of the empirical network, a saturation process apparently slows down the dynamics. We deal with this problem by using the network size instead of physical time as the measure of the course of the evolution, which allows us to compare the topology of the model and the empiric network despite its ongoing evolution [51].

The results of our model show the emergence of a dynamical phase transition from a disconnected to a connected state. The position of the critical point is related to the parameters λ and μ. For a fixed λ, increasing μ leads to the creation of more new disconnected components while the rate at which they are merged by the viral mechanism is kept constant; hence, the phase transition occurs at larger system sizes. Higher λ, however, increases the system's tendency to connect previously disconnected components, which leads to an earlier transition. We take advantage of the uniqueness of the critical point to adjust the parameters of the model by matching the network size of the model and the empiric network at the transition point. To this end, we compute the critical size for different values of the parameters λ and μ, as shown in Fig. 3. In the empiric network, the phase transition occurs at $N_c^P = 10600$, which is represented by the black contour line in the plot. The green line shows a linear fit according to
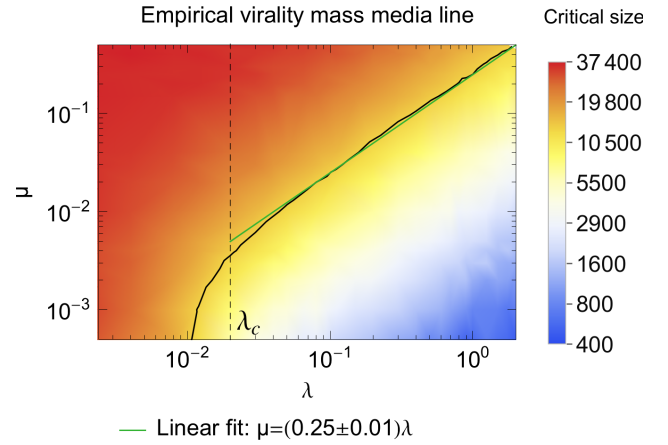
$$\mu(\lambda) = (0.25 \pm 0.01)\lambda. \tag{1}$$

FIG. 3. The color density plot represents the network size at the critical point for the respective parameters λ and μ. For constant λ, an increase of μ leads to a later transition (red area), whereas for constant μ, one observes an earlier transition (blue area) for higher values of λ. The solid black line indicates the virality mass media line corresponding to the critical size of Pokec ($N_c^P = 10600$). The green line shows a linear fit in the region above the sustained activity threshold $\lambda_c = 0.02$ (see Supplemental Material [39]).

The virality mass media line given by Eq. (1) quantifies the balance between the importance of the viral effect and the mass media effect for the evolution of the network. In light of this result, we conclude that the viral effect is about 4 times stronger than the mass media effect. In other words, in the particular case of the Pokec OSN, it is 4 times more likely to subscribe to the network as a result of a friend's invitation than as the result of the information about the network available through the mass media. However, Eq. (1) holds only above a critical value of the virality parameter $\lambda > \lambda_c$, which corresponds to the critical threshold for the self-sustained activity of the network (see Supplemental Material [39]). Below this limit, the virality mass media line bends downwards and, in the limit of $\lambda = 0$, it is not possible to match the position of the critical size (see Supplemental Material [39]). This implies that both virality and mass media influence are necessary and complementary mechanisms to explain the topological evolution of OSNs.

In the active phase, the effect of changing the value of λ is very mild if the relation Eq. (1) is preserved. In our case, we choose the value of λ that best reproduces the evolution of the number of disconnected components [Fig. 5(a)] and obtain the corresponding μ from Eq. (1). We then compare the results of the model with the empirical evolution of the Pokec OSN in Fig. 4. Interestingly, our two-parameter model is able to reproduce the entire evolution of the network with an impressive precision for all measured global topological properties, such as the size of the giant component, the ASPL, and the size of the second largest connected component; see Fig. 4. However, the model is
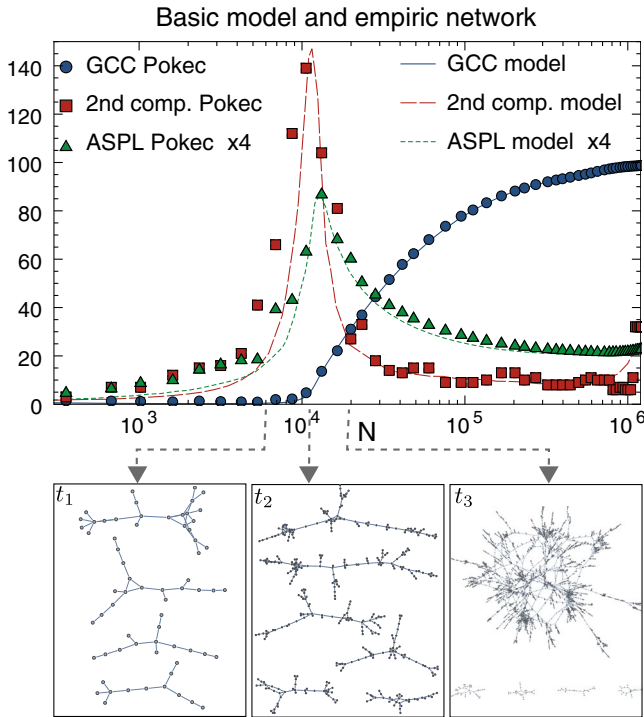
FIG. 4. Comparison of model and Pokec network evolution. Top: The symbols represent the empirical data, whereas the solid lines correspond to the results from the model averaged over 100 realizations with $\lambda = 0.03$ and $\mu = 0.008$. Points correspond to the empiric network and lines represent the results from the model. Bottom: Snapshots of the topology of the model at different times, similar to Fig. 1.
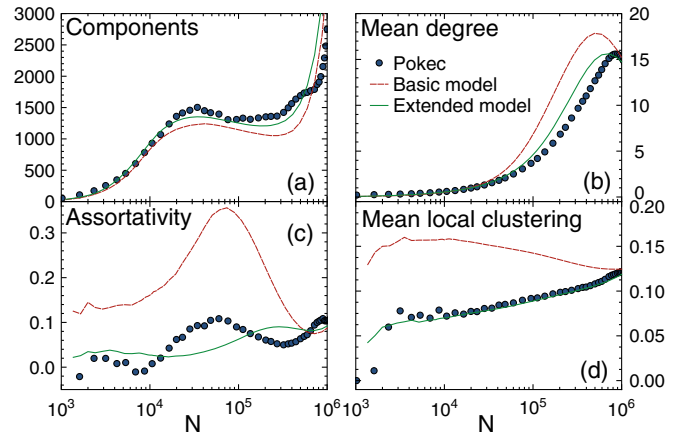

FIG. 5. Topological evolution of the empiric network (blue circles), the basic model (red dashed lines), and the extended model (green lines). (a) Evolution of the number of components of size $s > 1$. (b) The evolution of the mean degree shows a densification of the network. (c) The assortativity coefficient as defined in Ref. [52]. (d) The evolution of the mean local clustering coefficient (of nodes with $k > 1$) exhibits an essential difference between the basic model (red dashed line) and the extended model with $\eta = -0.65$ (green line).

not able to reproduce the temporal trends of local quantities, such as the mean local clustering and assortativity coefficients, as shown in Figs. 5(c) and 5(d). The clustering coefficient of the Pokec OSN steadily increases since the beginning of the evolution, whereas the model exhibits first a sudden increase followed by a decreasing clustering coefficient. The assortativity coefficient fluctuates both in the model and in the empiric network, although its value in the model is about 3 times higher. This disagreement suggests that a local mechanism must be incorporated to reproduce simultaneously the global and local evolution of the network topology. In the next section, we present an extended version of our model that takes into account the overlap of each node's neighborhood, with interesting implications concerning the strength of weak ties paradigm.

C. Extended model: Strong versus weak ties

The viral activation mechanism of our model is completely blind to the network topology; that is, active users try to "infect" all their neighbors with the same probability. As a consequence, the model performs well at reproducing the evolution of the global topological quantities, but it fails at reproducing trends in local quantities, like the clustering coefficient. However, according to Granovetter [20], the

diffusion of information through a social tie is different depending on whether the tie is "strong" or "weak." Following Granovetter's idea, we use the overlap of two individuals' friendship network as a measure of the strength of their tie [20]. In particular, given an edge connecting users i and j, we define its social strength as

$$s_{ij} \equiv (m_{ij} + 1), \qquad (2)$$

where m_{ij} counts the number of triangles going through the edge or, equivalently, the number of common neighbors of the two users.

Our previous model can now be easily extended to account for the strength of social ties. We assume that viral activation and reactivation through the edge $i \leftrightarrow j$ is given by

$$\lambda_{ij} = \lambda \frac{s_{ij}^{\eta}}{\langle s^{\eta} \rangle}, \qquad (3)$$

where $\langle \rangle$ denotes the global average over the whole network. In this way, the parameter λ has the same interpretation as in the basic model. The transmissibility-strength coefficient η represents the relationship between the viral transmissibility and the strength of the social tie. When $\eta > 0$, viral transmissibility is proportionally to the strength of social ties, which puts special emphasis on the strong ties for the viral spreading. Instead, when $\eta < 0$, the highest viral transmissibilities are assigned to edges with low multiplicities, which tend to act like connectors between different clustered groups (see Fig. 6). In the case of $\eta = 0$,
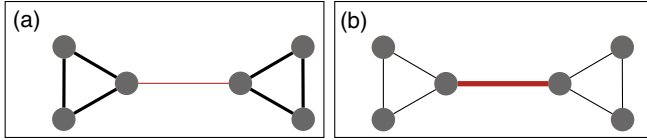
FIG. 6. (a) Illustration of the strength of social ties defined by Eq. (2). (b) Illustration of viral transmissibilities for negative η defined by Eq. (3).

we have $\lambda_{ij} = \lambda$, and we recover the basic model discussed in the previous section.

We quantify the transmissibility-strength coefficient η by comparing the evolution of the mean local clustering coefficient in the Pokec OSN with results from the extended model. Figure 5(d) shows that the clustering coefficient of the Pokec OSN grows approximately linearly with the logarithm of the network size. Thus, we interpolate the evolution of the clustering coefficient of our model for different values of η and compare the obtained slopes with the empirical one, as shown in Fig. 7. The extended model exhibits an increasing clustering coefficient for $\eta < -0.2$ [see Fig. (d)], and the best match with the Pokec OSN is achieved at the value of $\eta = -0.65$, which is, remarkably, a negative value. This is yet another empirical proof of Granovetter's theory of the importance of weak ties in processes of diffusion of information in social networks [20]. An alternative empirical validation of the same principle was provided in Ref. [25], where it was found that the probability of accepting an invitation to join an OSN is not proportional to the number of social contacts of the invited individual but to the number of different social contexts—the structural diversity—within the individual's
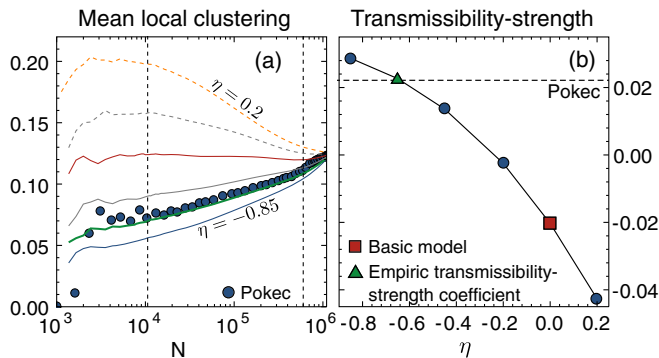

FIG. 7. (a) Evolution of the mean local clustering coefficient for different values of η from -0.85 to 0.2. The lines correspond to model results for different η and the symbols represent the evolution from the empiric network. We set $\lambda = 0.03$ and $\mu = 0.006$. (b) Slopes of the evolution of the mean local clustering coefficient for different values of the transmissibility-strength coefficient. The dashed line represents the slope of the clustering evolution of the Pokec network. The empirical transmissibility-strength coefficient $\eta = -0.65$ is given by the intersection of this line with the curve representing the model results.

life. Notice that a similar effect is achieved in our model when the exponent η is negative. Indeed, suppose that a user has a subset of k contacts forming a "strong" context, that is, these k contacts are all connected among them. This implies that the multiplicity of each link between our user and their k contacts is $m = k - 1$. Suppose now that $\eta = -1$, then the aggregated infectivity according to Eq. (3) is proportional to $k/(m+1) = \text{const}$, which is precisely the main result in Ref. [25].

The introduction of weighted transmissibilities in our model does not affect significantly the evolution of the global topological properties. Indeed, for $\eta = -0.65$, the virality mass media line behaves as it does in the basic model with the difference that now the relation between λ and μ is

$$\mu(\lambda) \approx (0.21 \pm 0.01)\lambda. \qquad (4)$$

As for the rest of the topological measures, the evolution of the GCC, the size of the second largest connected component, the ASPL, and the diameter are basically identical to the case of the basic model and are shown in the Supplemental Material [39]. In Fig. 5, we show results for the number of components, the mean degree, the assortativity coefficient, and the mean local clustering, which are all in very good agreement with their empirical counterparts.

III. DISCUSSION

Comprehensive data sets on the evolution of OSNs offer us the opportunity to determine the principal mechanisms involved in social contagion and online activity of individuals. In this respect, the OSN Pokec, with its peculiar evolution and being almost isolated, is particularly appropriate. Interestingly, the evolution of Pokec's topology is characterized by a dynamical percolation transition, a rather peculiar behavior in real evolving networks. We show that this anomalous topological evolution can be explained very precisely on a quantitative level by a two-layer model, which accounts for the underlying real social structure, combined with two main mechanisms. First, a viral effect, responsible for the social contagion of new users and, second, a mass media effect, leading to random subscriptions of new users. Interestingly, the balance between these two mechanisms is what governs the topological growth of OSNs. In the particular case of the OSN Pokec, the quantification of this balance tells us that the viral effect is between 4 and 5 times stronger than the mass media effect. This can explain the proliferation of viral marketing campaigns, in detriment of traditional advertising [1]. To our knowledge, for the first time a model with only very few parameters yields quantitatively precise insight about the topological formation of OSNs. This makes our model a necessary foundation for the development of next-generation online social networking services.

Beyond the global behavior of our basic model, the social neighborhood of individuals has shown to be crucial to explain the evolution of local topological quantities in Pokec. We find that viral transmissibility is inversely proportional to the strength of social ties. This result is particularly interesting as it corroborates recent empirical findings concerning the role of "structural diversity" on social contagion processes by analyzing Email invitations from Facebook users [25]. However, our model allows us to identify and quantify this effect exclusively from—and hence its impact on thee topological evolution of the OSN. Alongside Granovetter's conclusion about the importance of weak ties for individual success, our results give rise to the interpretation that OSNs evolve in a way to improve the possibilities for individual success. This might constitute an important reason for the huge popularity of OSNs.

Our findings here suggest interesting future research lines. Indeed, the particular OSN analyzed in this paper is a quasi-isolated system and, thus, allows us to gauge the fundamental mechanisms at play in the evolution of OSNs. However, in a general situation, an entire ecosystem of OSNs operate simultaneously, competing for the same users, which now become a scarce resource. The introduction of competition among OSNs in our model opens the possibility to develop an ecological theory of the digital world.

ACKNOWLEDGMENTS

[1] J. Leskovec, L. A. Adamic, and B. A. Huberman, *The Dynamics of Viral Marketing*, ACM Trans. Web **1,** 5 (2007).

[2] M. Richardson and P. Domingos, in *Proceedings of the Eighth ACM SIGKDD International Conference on Knowledge Discovery and Data Mining, KDD'02* (ACM, New York, 2002), pp. 61–70.

[3] J. L. Iribarren and E. Moro, *Branching Dynamics of Viral Information Spreading*, Phys. Rev. E **84,** 046116 (2011).

[4] J. L. Iribarren and E. Moro, *Impact of Human Activity Patterns on the Dynamics of Information Diffusion*, Phys. Rev. Lett. **103,** 038702 (2009).

[5] T.-A. Hoang and E.-P. Lim, *Virality and Susceptibility in Information Diffusions*, in *Proceedings of the Sixth International AAAI Conference on Weblogs and Social Media, 2012* (AAAI, Palo Alto, CA, 2012).

[6] L. K. Hansen, A. Arvidsson, F. Årup Nielsen, E. Colleoni, and M. Etter, *Future Information Technology*, Communications in Computer and Information Science Vol. 185 (Springer, Berlin, 2011), pp. 34–43.

[7] P. A. Grabowicz, J. J. Ramasco, E. Moro, J. M. Pujol, and V. M. Eguiluz, *Social Features of Online Networks: The Strength of Intermediary Ties in Online Social Media*, PLoS One **7,** e29358 (2012).

[8] D. G. Rand, S. Arbesman, and N. A. Christakis, *Dynamic Social Networks Promote Cooperation in Experiments with Humans*, Proc. Natl. Acad. Sci. U.S.A. **108,** 19 193 (2011).

[9] A. Ross and B. Scott, *Social Media: Cause, Effect and Response*, in NATO Review Magazine, 2011, http://www.nato.int/docu/review/2011/Social_Medias/21st-century-statecraft/EN/index.htm.

[10] A. Ordanini, *Crowd-Funding: Transforming Customers into Investors through Innovative Service Platforms*, Journal of customer service in marketing and management **22,** 443 (2011).

[11] iSocial: Decentralized Online Social Networks project, http://isocial-itn.eu/.

[12] A. Mislove, M. Marcon, K. P. Gummadi, P. Druschel, and B. Bhattacharjee, in *Proceedings of the 7th ACM SIG-COMM Conference on Internet Measurement, IMC'07* (ACM, New York, 2007), pp. 29–42.

[13] Y.-Y. Ahn, S. Han, H. Kwak, S. Moon, and H. Jeong, in *Proceedings of the 16th International Conference on World Wide Web, WWW'07* (ACM, New York, 2007), pp. 835–844.

[14] J. Ugander, B. Karrer, L. Backstrom, and C. Marlow, *The Anatomy of the Facebook Social Graph*, arXiv:1111.4503.

[15] S. Milgram, *The Small World Problem*, Psychol. Today **1,** 61 (1967).

[16] J. Travers, S. Milgram, J. Travers, and S. Milgram, *An Experimental Study of the Small World Problem*, Sociometry **32,** 425 (1969).

[17] M. Newman, A.-L. Barabási, and D. J. Watts, *The Structure and Dynamics of Networks* (Princeton University Press, Princeton, 2006).

[18] R. Albert, H. Jeong, and A. L. Barabasi, *The Diameter of the World Wide Web*, Nature (London) **401,** 130 (1999).

[19] J. Kleinberg, *Advances in Neural Information Processing Systems (NIPS) 14* (MIT Press, Cambridge, MA, 2001), p. 2001.

[20] M. S. Granovetter, *The Strength of Weak Ties*, Am. J. Sociology **78,** 1360 (1973).

[21] N. Friedkin, *A Test of Structural Features of Granovetter's Strength of Weak Ties Theory*, Soc. Networks **2,** 411 (1980).

[22] L. Lü and T. Zhou, in *Proceedings of the 1st ACM International Workshop on Complex Networks Meet Information, CNIKM'09* (ACM, New York, 2009), pp. 55–58.

[23] J.-P. Onnela, J. Saramäki, J. Hyvönen, G. Szabó, D. Lazer, K. Kaski, J. Kertész, and A.-L. Barabási, *Structure and Tie Strengths in Mobile Communication Networks*, Proc. Natl. Acad. Sci. U.S.A. **104,** 7332 (2007).

[24] M. Szell, R. Lambiotte, and S. Thurner, *Multirelational Organization of Large-Scale Social Networks in an Online World*, Proc. Natl. Acad. Sci. U.S.A. **107,** 13 636 (2010).

[25] J. Ugander, L. Backstrom, C. Marlow, and J. Kleinberg, *Structural Diversity in Social Contagion*, Proc. Natl. Acad. Sci. U.S.A. **109**, 5962 (2012).

[26] R. Kumar, J. Novak, and A. Tomkins, in *Proceedings of the 12th ACM SIGKDD International Conference on Knowledge Discovery and Data Mining, KDD'06* (ACM, New York, 2006), p. 611.

[27] H. Hu and X. Wang, *Evolution of a Large Online Social Network*, Phys. Lett. A **373**, 1105 (2009).

[28] H.-B. Hu and X.-F. Wang, *Disassortative Mixing in Online Social Networks*, Europhys. Lett. **86**, 18003 (2009).

[29] M. Li, S. Guan, X. Gong, K. Li, J. Wu, Z. Di, and C.-h. Lai, *From Sparse to Dense and from Assortative to Disassortative in Online Social Networks*, Sci. Rep. **4**, 4861 (2014).

[30] L. Maria Aiello, A. Barrat, C. Cattuto, G. Ruffo, and R. Schifanella, in *Proceedings of the 2010 IEEE Second International Conference on Social Computing* (IEEE, New York, 2010), pp. 249–256.

[31] G. F. Frasco, J. Sun, H. D. Rozenfeld, and D. ben-Avraham, *Spatially Distributed Social Complex Networks*, Phys. Rev. X **4**, 011008 (2014).

[32] J. L. Toole, M. Cha, and M. C. González, *Modeling the Adoption of Innovations in the Presence of Geographic and Media Influences*, PLoS One **7**, e29528 (2012).

[33] J. Leskovec, J. Kleinberg, and C. Faloutsos, *Graph Evolution: Densification and Shrinking Diameters*, ACM Trans. Knowl. Discov. Data **1**, 2 (2007).

[34] J. Leskovec, J. Kleinberg, and C. Faloutsos, in *Proceedings of the Eleventh ACM SIGKDD International Conference on Knowledge Discovery in Data Mining, KDD'05* (ACM, New York, 2005), pp. 177–187.

[35] L. Takac and M. Zabovsky, *Data Analysis in Public Social Networks*, in *Proceedings of the International Scientific Conference and International Workshop Present Day Trends of Innovations, Lomza, Poland, 2012*, http://scholar.google.com/citations? view_op=view_citation&citation_for_view=EzaFJ8oAAAAJ: WF5omc3nYNoC.

[36] J. C. González-Avella, M. G. Cosenza, and M. San Miguel, *A Model for Cross-Cultural Reciprocal Interactions through Mass edia*, PLoS One **7**, e51035 (2012).

[37] M. De Domenico, A. Solé-Ribalta, E. Cozzo, M. Kivelä, Y. Moreno, M. A. Porter, S. Gómez, and A. Arenas, *Mathematical Formulation of Multilayer Networks*, Phys. Rev. X **3**, 041022 (2013).

[38] The distribution of sizes of disconnected components at this point is a power law, another clear indication of the presence of a continuous phase transition; see Supplemental Material [39].

[39] See Supplemental Material at http://link.aps.org/ supplemental/10.1103/PhysRevX.4.031046 for additional information and plots.

[40] A.-L. Barabási and R. Albert, *Emergence of Scaling in Random Networks*, Science **286**, 509 (1999).

[41] S. N. Dorogovtsev, J. F. F. Mendes, and A. N. Samukhin, *Size-Dependent Degree Distribution of a Scale-Free Growing Network*, Phys. Rev. E **63**, 062101 (2001).

[42] G. Bianconi and A.-L. Barabási, *Bose-Einstein Condensation in Complex Networks*, Phys. Rev. Lett. **86**, 5632 (2001).

[43] G. Caldarelli, A. Capocci, P. De Los Rios, and M. A. Muñoz, *Scale-Free Networks from Varying Vertex Intrinsic Fitness*, Phys. Rev. Lett. **89**, 258702 (2002).

[44] A. Vázquez, *Growing Network with Local Rules: Preferential Attachment, Clustering Hierarchy, and Degree Correlations*, Phys. Rev. E **67**, 056104 (2003).

[45] R. Pastor-Satorras, E. Smith, and R. V. Sole, *Evolving Protein Interaction Networks through Gene Duplication*, J. Theor. Biol. **222**, 199 (2003).

[46] S. Fortunato, A. Flammini, and F. Menczer, *Scale-Free Network Growth by Ranking*, Phys. Rev. Lett. **96**, 218701 (2006).

[47] R. M. D'Souza, C. Borgs, J. T. Chayes, N. Berger, and R. D. Kleinberg, *Emergence of Tempered Preferential Attachment from Optimization*, Proc. Natl. Acad. Sci. U.S.A. **104**, 6112 (2007).

[48] F. Papadopoulos, M. Kitsak, M. Serrano, M. Boguñá, and D. Krioukov, *Popularity versus Similarity in Growing Networks*, Nature (London) **489**, 537 (2012).

[49] R. M. Anderson and R. M. May, *Infectious Diseases in Humans* (Oxford University Press, Oxford, England, 1992).

[50] B. Ribeiro, in *Proceedings of the International World Wide Web Conference, Seoul, WWW'14* (ACM, New York, 2014).

[51] This corresponds to dynamically rescaling λ, μ, and δ in the same way at each time step. Hence, the transformation preserves the fraction λ/μ, which we discuss in terms of the balance between virality and mass media influence.

[52] M. Newman, *Networks: An Introduction* (Oxford University Press, New York, 2010).